HHS Public Access

Author manuscript

Kidney Int. Author manuscript; available in PMC 2014 November 01.

Published in final edited form as:

Kidney Int. 2014 May ; 85(5): 1091–1102. doi:10.1038/ki.2013.433.

Early B cell factor 1 is an essential transcription factor for postnatal glomerular maturation

Jackie A. Fretz[1], **Tracy Nelson**[1], **Heino Velazquez**[2], **Yougen Xi**[1], **Gilbert Moeckel**[3], and **Mark C. Horowitz**[1]

[1]Department of Orthopaedics and Rehabilitation, Yale University School of Medicine, New Haven, CT 06520, USA

[2]Department of Internal Medicine- Nephrology, Yale University School of Medicine, New Haven, CT 06520, USA

[3]Department of Pathology, Yale University School of Medicine, New Haven, CT 06520, USA

Abstract

The coordination of multiple cytokines and transcription factors with their downstream signaling pathways have been shown to be integral to nephron maturation. Here we present a completely novel role for the helix-loop-helix transcription factor Early B cell Factor 1 (Ebf1), originally identified for B cell maturation, for the proper maturation of glomerular cells from mesenchymal progenitors. The expression of Ebf1 was both spatially and temporally regulated within the developing cortex and glomeruli. Using Ebf1-null mice we then identified biochemical, metabolic, and histological abnormalities in renal development that arose in the absence of this transcription factor. In the Ebf1 knockout mice the developed kidneys show thinned cortices and reduced glomerular maturation. The glomeruli showed abnormal vascularization and severely effaced podocytes. The mice exhibited early albuminuria and elevated blood urea nitrogen levels. Moreover, the GFR was reduced over 66 percent and the expression of podocyte-derived VEGF-A was decreased compared to wild type control mice. Thus, Ebf1 has a significant and novel role in glomerular development, podocyte maturation, and the maintenance of kidney integrity and function.

Introduction

Early B cell factor 1 (Ebf1) is the founding member of a unique class of helix-loop-helix transcription factors (TFs) (1). They are thought to bind as homo or heterodimers to a recognition sequence containing two considerably degenerate 6 bp half sites separated by a 2 bp spacer (2–4). Originally, Ebf1 was found to be necessary for B cell maturation as progenitors deficient in its expression arrested at the pre-pro-B cell stage (2). Ebf1 has since

Contact: Jackie A. Fretz, Ph.D., Yale University, School of Medicine, PO Box 208071 (MORTHO), New Haven, CT 06520-8071, 203-785-5930 (p), 203-737-2529 (f), jackie.fretz@yale.edu.

Disclosure:
The authors state that they have nothing to disclose.

been identified by our laboratory and others as an important TF for proper differentiation of adipocytes and osteoblasts from mesenchymal progenitors (5–7).

Many TFs have been shown to be important for different stages of podocyte maturation. Wt1 is the earliest marker of the podocyte, and depending upon the degree of Wt1 deficiency a spectrum of kidney defects can arise from adult-onset nephrotic syndrome to complete renal agenesis in $Wt1^{-/-}$ animals (8–11). Loss of Pod-1 or Mafb arrests glomeruli at the single capillary loop stage (12, 13), while Foxc2-null mice have abnormally shaped glomeruli containing fewer and dilated capillary loops (14). Podocytes deficient in Lmx1b fail to develop foot processes and have defective basement membrane formation (15).

We initially investigated a role for Ebf1 in kidney maturation during exploration of the mechanism underlying the bone phenotype of Ebf1-deficeint mice. We present here the first report of a functional role for any Ebf-family protein in kidney. Unique among its family members, Ebf1 is expressed dynamically during late kidney organogenesis and in its absence organs manifest with significant perturbations of morphology and function. The most prominent of these developmental defects is a dramatic reduction in late glomerular maturation, which appears to involve mis-regulation of VEGF-A production from podocytes subsequently leading to proteinuria and decreased glomerular filtration rate (GFR). We conclude that similar to those TFs mentioned above, Ebf1 is also an essential regulator of podocyte differentiation and glomerular maturation.

Results

Ebf1-deficient mice have decreased GFR

While examining Ebf1's role in osteoblast function (6) we identified an incongruity between the quality of bone, and the level of circulating osteocalcin (Ocn). Ocn is an osteoblast-specific protein that constitutes the major non-collagenous matrix protein in bone, and measurement of circulating Ocn is a long established clinical indicator of osteoblastic activity and bone mineral density (16). While serum Ocn of *Ebf1*$^{-/-}$ mice was twice that of their littermates (Fig. 1A) the *Ebf1*$^{-/-}$ mice had low bone mineral density (6, 17), and their osteoblasts displayed a markedly reduced ability to induce Ocn mRNA during differentiation *in vitro* (Fig. 1B) and *in vivo* (Fig. 1C). (A detailed description of the mechanisms underlying this defect in osteoblast maturation will be published elsewhere.)

The major route of clearance for Ocn is the kidney, and its circulating levels correlate inversely with decreased renal function where it can be 2–200xs higher than levels in healthy individuals (18–22). To determine if decreased renal clearance was affecting circulating Ocn in *Ebf1*$^{-/-}$ mice we examined GFR through administration of radio-labeled inulin. The observed GFR revealed an 80% reduction in kidney function in *Ebf1*$^{-/-}$ mice compared to their controls (Fig. 1D). Ebf1-deficient mice are smaller than their littermates (*Ebf1*$^{+/+}$ = 17.5 ± 0.9g, *Ebf1*$^{-/-}$ = 7.5 ± 0.3g) so a slight reduction in GFR is expected based upon the need for allometric scaling. However, even after adjusting for body size (Fig. 1D, expected values) (23), the GFR of *Ebf1*$^{-/-}$ animals was reduced by more than 66%, while the values from *Ebf1*$^{+/+}$ littermates did not differ. Labeled inulin also accumulated in the plasma of *Ebf1*$^{-/-}$ mice (Fig. 1E). Changes were not observed for any other marker of

physiological function except for a small increase in heart rate, which may be contributable to their reduced size (Fig. 1F,G).

The health of the animals was next assessed. Serum analysis revealed elevated BUN in the *Ebf1*$^{-/-}$ mice by P28 (Fig. 1H). Serum creatinine was not dramatically elevated at P28 (Fig. 1I). Creatinine is, however, influenced by muscle mass and body size and becomes an unreliable predictor in situations with large differences in muscle mass are observed (24). Therefore, changes in filtration may not be accurately measured by analysis of creatinine by the smaller body size of the *Ebf1*$^{-/-}$ animals. However, by P90, even with runted appearance of Ebf1$^{-/-}$ mice, significant elevations in serum creatinine are detectable (Fig. 1I). Urinalysis revealed albuminuria manifesting around P14 that progressed with age (Fig. 1J,K). Accordingly, serum albumin is low by P28 in *Ebf1*$^{-/-}$ animals (Fig. 1L). The expression of lipocalin2, an early and sensitive marker of nonspecific kidney damage, also correlated with the onset of albuminuria (Fig. 1M).

Histological Examination of *EBF1*$^{-/-}$ Kidney

Having observed a decrease in renal function, we next examined the kidneys for morphological changes. While kidneys were not significantly smaller for the reduced size of the *Ebf1*$^{-/-}$ mice (Fig. 2A), they were paler, and displayed alterations in their histological anatomy (Fig. 2B–F). The cortex was thinned by 60%. The outer medulla was also thinned, almost completely lacking the outer stripe, and had disorganized medullary arrays and a paucity of vascular bundles in the inner stripe. In contrast, the inner medulla and papilla were largely unaffected. Most striking was the persistence of islands containing vimentin-positive cells and dysmorphic glomeruli along the peripheral cortex of *Ebf1*$^{-/-}$ kidneys (Fig. 2E and Supplemental Fig. 1). While glomeruli in the juxtamedullary (JM) region were relatively mature with multiple capillary loops, the glomeruli within these undifferentiated regions appeared hypomorphic (Fig. 2F).

The majority of *Ebf1*$^{-/-}$ mice die of unknown etiology at or before 3 months of age; rarely do animals live much longer than 3 months. Examination of kidneys from 2 and 3-month-old mice revealed a worsening of the metanephric phenotype with pronounced tubular lumen dilation, accumulation of tubular proteinaceus casts with scalloped edges, and schistocytes in the urinary space (Fig. 2G–K). Hypomorphic glomeruli still persist in the periphery (Fig. 2I). At 2 months some glomeruli in the JM region of *Ebf1*$^{-/-}$ mice appear lobulated but overall do not exhibit extensive hypercellularity or sclerosis until the animals are about 3 months old (Fig. 2J). Modest interstitial fibrosis is also apparent in the older Ebf1-deficient animals (Fig. 2K).

Ebf1 expression is induced postnatally

The expression of Ebf1, or any Ebf family members, has not been directly examined in kidney. A recent gene-chip study focusing on the differentiation of different endothelial cell types in the developing kidney identified Ebf1 as one of the genes whose expression was strongly up-regulated during endothelial differentiation (25). Freely available *in situ* hybridization (ISH) in E14.5 kidney (www.genepaint.org) localized Ebf1 to condensed mesenchyme that has begun to initiate nephrogenesis (26). This expression pattern is unique

among its family members; Ebf2 was expressed ubiquitously throughout the developing organ while Ebf3 was only in the capsule and Ebf4 was not present (26).

We began our analysis of Ebf1 expression in the postnatal kidney by first examining the RNA expression profiles of all four Ebf family members in whole kidneys of P28 mice (Fig. 3A). As was observed in the embryonic mouse, transcripts for both Ebf1 and Ebf2 were detected in adult kidney. Ebf3 and Ebf4 messages were either marginally detectable or not present. Ebf1-knockout animals also do not appear to compensate for the loss of Ebf1 by attempting to up-regulate expression by other Ebf family members. We next examined whether distribution of Ebf1 changed over time. At P4, while Ebf1 was present in some tubules, it was absent from any population of the glomerulus (Supplemental Fig. 1B). During postnatal metanephric development, Ebf1 was strongly up-regulated in all components of the cortex as time progressed (Fig. 3B). IF of Ebf1 protein expression showed expanding expression over time (Fig. 3C), and Ebf1 appeared within the podocytes by P14 (Fig. 3C). This expression pattern was maintained into adulthood (P28). To confirm expression of Ebf1 in the podocyte, primary podocytes were cultured from isolated glomeruli and cell lysate was analyzed by western blot (Fig. 3D, purity of the isolated podocytes is verified in Supplemental Fig. 2). While Ebf1 was not detected in the podocyte lysate from P2 animals, it was present when cells were isolated from P14 animals. This was further confirmed by IF co-staining of cultured podocytes for Wt1 and Ebf1 (Fig. 3E). This expression data explains why peripheral glomeruli are more severely affected than those that develop more JM prior to the induction of Ebf1 within this population *in vivo*.

Ebf1 abrogates tuft development though podocyte-mediated processes

Tuft formation and mesangial migration are intimately linked in podocyte development (27). Without an initial influx of endothelial cells into the vascular space, a mesangial stalk will not form. Conversely, without mesangial cells or a glomerular basement membrane (GBM) that supports mesangial adherence looping of glomerular capillaries will not proceed past the capillary loop stage (28, 29). While the Bowman's spaces of the hypomorphic glomeruli are formed their tufts exhibited a paucity of delicate capillary development compared to controls. Quantification revealed a 40–85% decrease in the number of capillary loops per glomeruli in *Ebf1*$^{-/-}$ mice depending upon the location of the developing glomerulus (Fig. 4A). In general, there was not significant expansion of the urinary space in any region of the cortex, but perfusion fixation did result in distention of select structures at a low rate (1–2 glomeruli per section) (Supplemental Fig. 3). Analysis of the cross-sectional surface area per glomeruli also showed decreased glomerular development after P14 but not prior (Fig. 4B). Immunofluorescent (IF) staining of both capillary endothelial cells and mesangium confirmed that poorly formed peripheral glomeruli from *Ebf1*$^{-/-}$ kidneys exhibited reduced numbers of mesangial cells and less developed capillary networks (Fig. 4C). This was also seen through RNA analysis of endothelial and mesangial transcripts in whole kidney, which show reduced expression from postnatal day 14 (P14) onward (Fig. 4D).

Transmission electron microscopy (TEM) was next performed. Glomeruli from P28 animals, regardless of glomerular location within the cortex and extent of glomerular development, were found to be extensively effaced (Fig. 5A). Podocytes were also found in

apical contact with the Bowman's capsule (Fig. 5A). The majority of the GBM was relatively normal without evidence of immune complex deposits, but there was some segmental thickening and multi-lamellation (Fig. 5A). These GBM alterations only occurred adjacent to completely effaced podocytes. The endothelial cells were also affected at these sites and exhibited disruption and loss of their characteristic fenestrations (Fig. 5A).

As glomeruli appear to form relatively normally before Ebf1 is expressed we next examined if foot processes were ever present in podocytes of *Ebf1*$^{-/-}$ mice. When P0 kidneys were examined by TEM (Fig. 5B) no differences in foot process formation could be observed between genotypes. This indicates that foot processes do form in the podocytes of *Ebf1*$^{-/-}$ JM glomeruli prior to Ebf1 induction, and that effacement is either a secondary response to their increased filtration load in the absence of properly functioning peripheral glomeruli, or a failure to maintain foot processes once proper maturation is blocked in podocytes following P14.

During GBM maturation there is normally a shift in the composition of collagen IV fibrils and lamins integrated into the barrier (30). Mutations in components of the GBM, as well as their associated integrins, results in glomerular disease and podocytes that are unable to form or maintain proper foot processes (31–34). To address the GBM alterations observed with TEM, we examined glomeruli from *Ebf1*$^{-/-}$ mice for the production of late-stage collagen IV fibers. Here again, glomerular development appeared inhibited in the peripheral cortex at P14 with reduced integration of late-stage collagen IV trimers containing α3 fibers in both the hypomorphic peripheral glomeruli and more developed JM structures (Fig. 6A). RNA expression analysis of whole kidney supports a podocyte-mediated change in expression of these structural collagens (Fig. 6B).

Ebf1 functions late in Podocyte development and involves regulation of VEGF

Podocyte-derived production of vascular endothelial growth factor A (VEGF-A) directs migration of endothelial cells into the distal cleft of the S-shaped body to form capillaries in the developing glomeruli (35–37). The infiltrating endothelial cells produce platelet-derived growth factor (PDGF), which is essential for mesangial migration and to induce splitting of the capillary tuft to form the mature glomerulus (28, 38). The Ebf1-mediated defect appears to be relatively early in this process so we next examined podocyte-derived VEGF-A protein at P14 and P28. At both ages, poorly developed peripheral glomeruli exhibited reduced staining for VEGF within the corpuscle (Fig. 7A). One of the main regulators of VEGF-A in podocytes is Wt1 (39). Analysis of RNA from total kidney of P28 animals indicated that many direct targets of Wt1 show reduced expression (nephrin (Nphs1), podocalyxin (Podxl), VEGF-A (Vegfa)), while loss of repression was observed for other targets normally suppressed by Wt1 (Pdgf-α, Pax2)) (Fig. 7B). Transcript levels of Wt1 were also reduced at this age. IHC of P14 and P28 animals revealed Wt1 was present in both poorly developed peripheral glomeruli and more JM located structures of *Ebf1*$^{-/-}$ mice (Fig. 7C). Quantification of fluorescence intensity revealed equivalent expression of Wt1 in peripheral podocytes between genotypes at P14, but Wt1 was decreased in the JM *Ebf1*$^{-/-}$ glomeruli at P28 (Fig. 7D).

It is well known that an increased filtration load on healthy glomeruli results in damage-induced dedifferentiation of the podocytes and downregulation of Wt1. This appears to be plausible for the downregulation observed by P28 in JM *Ebf1*$^{-/-}$ glomeruli (Fig. 7D). Furthermore, both fluorescence intensity and Wt1-trancript levels from whole kidney are elevated in P14 Ebf1$^{-/-}$ kidneys (Fig. 7D,E) suggesting either a phenotype-mediated compensation of Wt1 expression once Ebf1 fails to be expressed, or a persistence of a more immature podocyte-lineage cell in the *Ebf1*$^{-/-}$ tissue with higher expression of Wt1 at p14 followed by compensatory down-regulation of Wt1 in filtration overload-damaged cells by P28. Additionally, when podocytes were isolated *in vitro* Wt1 transcript levels, and many Wt1 targets, were no longer mis-regulated including Neph1 and Pax2 (Fig. 7E). Others, like VEGF-A and Podxl were still down-regulated (Fig. 7E). Discrepancies in these changes may simply be a result of loss of the 3-dimensional architecture and foot processes as podocytes are grown in culture, or instead *in vivo* culture may be eliminating secondary effects that occur *in vivo*. Production of a separate podocyte-derived factor involved in endothelial cell recruitment, angiopoietin-1, also was not altered (Fig. 7F). Decreased VEGF-A occurs both *in vivo* and *in vitro* despite significant levels of Wt1, and suggests that maturation of the peripheral glomeruli is arrested due to a failure of *Ebf1*$^{-/-}$ podocytes to properly up-regulate VEGF-A and initiate epithelial and mesangial recruitment.

Other podocyte-related TFs, apart from Wt1, are integral to podocyte differentiation and have known roles in glomerular vascularization. To determine if Ebf1 is working upstream or downstream of these other TFs, we next examined the expression of Mafb, Pod-1, Foxc2, and Lmx1b in isolated *Ebf1*$^{-/-}$ podocytes (Fig. 7G). RNA from isolated podocytes from 3 week old animals revealed that while Mafb, and Foxc2 do not appear to be altered in their expression, Pod1 and Lmx1b transcripts were significantly reduced in the absence of Ebf1. Taken together these results demonstrate a novel function of Ebf1 where it is integral to late podocyte function and postnatal maturation of murine peripheral glomeruli.

Discussion

We report here the first observation of a role for Ebf1 in renal health. The most striking feature of Ebf1-deficiency in kidney is a defect in glomerular tuft development accompanied by podocyte-intrinsic changes in VEGF-A expression. This is a completely novel function of Ebf1, whose role in any kidney process had been previously unrecognized. While we have focused our observations on the mechanism and phenotype underlying glomerular maturation and the role of Ebf1 in podocytes, there are clearly phenotypic changes in other kidney cell types that are beyond the scope of this initial report. As Ebf1 appears to be strongly up-regulated throughout the entire cortex during the last stages of renal development, and in light of the significant role that paracrine factors play in the development of the nephron, future studies will have to evaluate how the loss of Ebf1 in other regions of the tubule contributes to the phenotype that we see in the global knockout.

Ebf1's expression pattern in the cortex, and particularly podocytes, is unique in that it is not regulated by a specific stage of cellular differentiation, but instead in a time-dependent manner by a cortex-wide signaling event. Thus, once Ebf1 fails to be expressed postnatally tuft development is arrested regardless of the stage of the developing glomerulus resulting in

the gradation of phenotype we observe across cortex depth. Why Ebf1 could be so integral to glomerular formation after P14, but not prior to this time is a surprising observation, and one for which we do not yet have a definitive answer. It is, however, well recognized that formation and function of the peripherally located cortical nephrons is quite different than those in a more JM position as evidenced by the longer loops of henle and larger glomeruli in the more JM structures (40). Species-specific differences in the percentages of long versus short looped nephrons suggest a genetic component to their development, but the mechanisms underlying these distributions is currently unknown. The shorter looped nephrons in the peripheral cortex turn in the outer medulla, and are also the nephrons most affected by deletion of Ebf1. Therefore, changes in the outer medulla may be mostly due to a reduction in the numbers of short looped nephrons in the periphery of Ebf1-deficient tissue.

Only one other mouse model has been reported to harbor similar depth-dependent changes in late kidney development to that of Ebf1. The Cox2-deficient mouse also displays hypomorphic cortical glomeruli between P10–14 and progressive outer cortical dysplasia (41). Cox2-null mice, however, have a much more fibrotic and cystic phenotype than is seen with *Ebf1*$^{-/-}$, and the pattern of Cox2 expression does not overlap with or change in a manner that correlates with Ebf1 (42). Considering the extent of the decreased filtration rate and developmental damage present in the *Ebf1*$^{-/-}$ tissue, it is somewhat surprising that there is relatively little fibrosis in these mice prior to 3 months of age. This may, however, be attributable their absence of B cells, as B cell-mediated processes contribute to the mechanism underlying kidney fibrosis (43, 44).

Nephrogenesis completes during late gestation in humans, and during the early postnatal period in rodents. Beyond these windows in time, formation of new nephrons is not possible. Yet, while chronic kidney disease involves progressive scarring, scarring is not always irreversible. Reversal of scarring in the glomerulus involves expansion of the capillary tuft and removal of excessive extracellular matrix. Obtaining a greater understanding of the processes underlying tuft formation and repair are currently areas of therapeutic interest for treatment of glomerular disease. Our findings suggest that the actions of Ebf1 within the podocyte are involved in regulation of this signaling axis during terminal glomerular differentiation and into adulthood. Furthermore, the data we present here supports the possibility that alterations in Ebf1 expression or promotor/enhancer occupancy by Ebf1 may be an underlying mechanism involved in progression or regression of glomerular damage.

It is difficult to separate secondary paracrine effects on glomerular maturation from the direct mechanism of Ebf1 in podocytes *in vivo.* This is particularly relevant regarding changes in Wt1 expression and Wt1-regulated genes *in vivo* vs. *in vitro.* Examination of podocytes *in vitro*, and prior to large filtration load-meadiated effects (P14) suggests that expression of VEGF-A and Podxl are regulated by the presence of Ebf1. This is in contrast to Wt1, many Wt1-regulated genes, Mafb and Foxc2, which are all expressed at levels equivalent to what is observed in littermate controls *in vitro* but not *in vivo.* Alterations in the expression of these transcripts observed *in vivo*, occurs in response to filtration-related dedifferentiation of podocytes and not the loss of Ebf1 directly.

In contrast to the TFs above, Pod1 and Lmx1b expression is dramatically reduced in the Ebf1-deficient podocytes *in vivo* and *in vitro*. Although Pod1 and Lmx1b are expressed prior to Ebf1 induction in the podocyte, it appears that maintenance of their expression during late stages of glomerular maturation is directly dependent upon, or secondary to, the function of Ebf1. Pod1 is first expressed in developing podocytes of the S-shaped body adjacent to the vascular cleft and is sustained through later stages of glomerular maturation until, and including, terminal differentiation (45). The expression of Lmx1b coincides with that of Pod1 and it has also been implicated in the maturation of tuft development (46, 47). Reduction in the expression of Pod1 and Lmx1b may be contributing to the phenotype we have observed. Although no reports have been made using a floxed-podocyte specific knockout of Pod1, Pod1 is thought to play an important role in remodeling and maturation of the glomerular vasculature (48). Lmx1b regulates many of the messages that appear to be altered in the Ebf1-deficient cells including VEGF-A, Collagen IV-α3 and Collagen IV-α4, and their expression was reduced in both null and heterozygous animals (15). No connection has been made between the expression of Podxl and Pod1 or Lmx1b, yet its expression was also significantly reduced *in vivo* and *in vitro* in the absence of Ebf1. Elucidation of whether the changes we observe in podocyte makers are primary or secondary mechanisms of the actions of Ebf1 are the focus of ongoing research.

In conclusion, we believe that the function of Ebf1 in renal development is not only significant for its role in cortical tuft development, but unique in its pattern of expression and late developmental phenotype. Future investigations to identify the transcriptional targets of Ebf1 in the podocyte will provide a greater understanding of the role of this key TF in development and maintenance of podocytes during kidney maturation and disease progression.

Materials and Methods

Mice

Ebf1$^{-/-}$ mice were originally generated by Dr. Rudolf Grosschedl (49). F2 *Ebf1*$^{-/-}$ and *Ebf1*$^{+/+}$ mice maintained on a mixed C57BL/6 and 129X1/SvJ background were used for all experiments (50). The Yale Medical School IACUC approved the purchase and use of all animals.

Serum Ocn

Ocn levels in the sera were measured by a standard equilibrium radioimmunoassay using specific goat anti-mouse Ocn antibody (51).

RT-qPCR

Cells or tissues were lysed in Trizol (Invitrogen) and either processed immediately, or flash frozen and stored at −80°C for later use. Tissue was homogenized and the total RNA was isolated following the manufacturer's instructions. 1 μg of RNA was reverse transcribed using qScript (Quanta) then analyzed by real time PCR (qPCR) on an ABI Step One machine, and amplified using Kapa Sybr Fast Universal. The values were normalized relative to the expression of L9.

GFR

After anesthetization the bladder, carotid artery and external jugular vein were catheterized. Following a saline bolus (1% body weight after surgical prep) ^{3}-H inulin was infused at 50 μCi per hour per mouse at a volume flow rate of 12 μl/g body wt/hr. After a 40 minute equilibration period, 2 sequential 30 minute urine samples were collected and the volume measured. Blood was sampled at the midpoint of each urine collection. Plasma or urine was pipetted into liquid scintillation fluid (Optifluor, PerkinElmer) and counted in a liquid scintillation counter.

Histology

For perfusion fixation animals were anesthetized and perfused briefly with PBS followed by a periodate-lysine-paraformaldehyde (PLP) solution. Alternately, tissues were fixed in 10% buffered formalin and embedded in paraffin before being sectioned and stained with hematoxylin and eosin (Sigma) or Gomori Trichrome (Sigma).

Serum and Urine Collection

For serum, blood was collected retroorbitally, and sera was separated by centrifugation. Urine collections were all spot urines. Albumin was measured by ELISA (Bethyl Labs). Total protein was measured by Bradford assay. Creatinine and BUN were measured by submitting samples to the Yale Mouse Metabolic Phenotyping Center (MMPC as fee for service).

TEM

Samples were prepared by PLP-fixation and submitted to the Renal Pathology and Electron Microscopy Laboratory at Yale. A Zeiss LIBRA 120 Electron Microscope was used to scan the specimens. Images were digitized from the electron microscope using the Advanced Microscopy Techniques (AMT) CCD Camera system and software.

ISH

Antisense cRNA probes directed against mouse *Ebf1* were generated and labeled with digitoxigenin-11-UTP (Roche). Incubation and Staining was performed as described previously (52).

Western Blot

Whole cell protein lysate was collected and 30 μg of lysate was separated by SDS-PAGE, transferred to nitrocellulose, blocked with IgG-free BSA and probed for Ebf1 (Santa Cruz, sc-15888). Secondary antibody was α-goat-HRP (Santa Cruz, sc-2033).

IF

Kidneys were collected bisected, and stored in OCT at −80°C. 8 μm frozen sections were cut, and samples were fixed according to the antibody requirements. Staining was performed as described previously (52). See Table S1 for antibodies and hybridization conditions. Fluorescence was preserved with ProLong Gold antifade reagent (Invitrogen). Quantification of signal intensity was calculated on sections co-stained on the same slide

and captured using identical exposures/parameters. ImageJ software was used to perform densitometric analysis.

Statistical Analysis

All values are expressed as mean±SE. We evaluated differences between groups through Student's two tailed t-test analysis. Significance is indicated (*) when $p \leq 0.05$.

Supplementary Material

Refer to Web version on PubMed Central for supplementary material.

Acknowledgments

Support: JAF is funded by NIH K99DK093711 (NIDDK). MCH is funded by AR052690, AR046032 and DK084970 from NIH (NIDDK and NIAMS). HV is funded by P30DK079310. GM is funded by an NIDDK RO3. The George M. O'Brien Kidney Center at Yale is funded by NIH P30DK079310. The Yale Renal Pathology & Electron Microscopy Laboratory and the Yale Core Center for Musculoskeletal Disorders are both supported by NIH P30 grants. The Mouse Metabolic Phenotyping Center at Yale is part of an NIH-supported Consortium (NIDDK).

We thank Caren Gundberg for Ocn measurements, Nancy Toriano and Christiane Coady at the Yale Core Center for Musculoskeletal Disorders (NIH P30) for expert histological assistance, Margaret Ionello and the Yale Renal Pathology & Electron Microscopy Laboratory (NIH P30) for assistance with TEM, Tong Wang and Patricia Presig at the George M. O'Brien Kidney Center at Yale (NIH P30DK079310) for help with vascular perfusion and measurement of GFR, and Lloyd Cantley for critical feedback and review of this manuscript. JAF is funded by NIH K99DK093711 (NIDDK). MCH is funded by AR052690, AR046032 and DK084970 from NIH (NIDDK and NIAMS). HV is funded by P30DK079310. GM is funded by an NIDDK RO3.

References

1. Liberg D, Sigvardsson M, Akerblad P. The ebf/olf/collier family of transcription factors: Regulators of differentiation in cells originating from all three embryonal germ layers. Mol Cell Biol. 2002; 22:8389–8397. [PubMed: 12446759]
2. Hagman J, Belanger C, Travis A, et al. Cloning and functional characterization of early b-cell factor, a regulator of lymphocyte-specific gene expression. Genes Dev. 1993; 7:760–773. [PubMed: 8491377]
3. Travis A, Hagman J, Hwang L, et al. Purification of early-b-cell factor and characterization of its DNA-binding specificity. Mol Cell Biol. 1993; 13:3392–3400. [PubMed: 8497258]
4. Wang SS, Tsai RY, Reed RR. The characterization of the olf-1/ebf-like hlh transcription factor family: Implications in olfactory gene regulation and neuronal development. J Neurosci. 1997; 17:4149–4158. [PubMed: 9151732]
5. Akerblad P, Lind U, Liberg D, et al. Early b-cell factor (o/e-1) is a promoter of adipogenesis and involved in control of genes important for terminal adipocyte differentiation. Mol Cell Biol. 2002; 22:8015–8025. [PubMed: 12391167]
6. Hesslein DG, Fretz JA, Xi Y, et al. Ebf1-dependent control of the osteoblast and adipocyte lineages. Bone. 2009; 44:537–546. [PubMed: 19130908]
7. Jimenez MA, Akerblad P, Sigvardsson M, et al. Critical role for ebf1 and ebf2 in the adipogenic transcriptional cascade. Mol Cell Biol. 2007; 27:743–757. [PubMed: 17060461]
8. Guo JK, Menke a L, Gubler MC, et al. Wt1 is a key regulator of podocyte function: Reduced expression levels cause crescentic glomerulonephritis and mesangial sclerosis. Hum Mol Genet. 2002; 11:651–659. [PubMed: 11912180]
9. Kreidberg JA, Sariola H, Loring JM, et al. Wt-1 is required for early kidney development. Cell. 1993; 74:679–691. [PubMed: 8395349]

10. Jeanpierre C, Denamur E, Henry I, et al. Identification of constitutional wt1 mutations, in patients with isolated diffuse mesangial sclerosis, and analysis of genotype/phenotype correlations by use of a computerized mutation database. Am J Hum Genet. 1998; 62:824–833. [PubMed: 9529364]
11. Schumacher V, Scharer K, Wuhl E, et al. Spectrum of early onset nephrotic syndrome associated with wt1 missense mutations. Kidney Int. 1998; 53:1594–1600. [PubMed: 9607189]
12. Quaggin SE, Schwartz L, Cui S, et al. The basic-helix-loop-helix protein pod1 is critically important for kidney and lung organogenesis. Development. 1999; 126:5771–5783. [PubMed: 10572052]
13. Imaki J, Onodera H, Tsuchiya K, et al. Developmental expression of maf-1 messenger ribonucleic acids in rat kidney by in situ hybridization histochemistry. Biochem Biophys Res Commun. 2000; 272:777–782. [PubMed: 10860830]
14. Takemoto M, He L, Norlin J, et al. Large-scale identification of genes implicated in kidney glomerulus development and function. Embo J. 2006; 25:1160–1174. [PubMed: 16498405]
15. Morello R, Zhou G, Dreyer SD, et al. Regulation of glomerular basement membrane collagen expression by lmx1b contributes to renal disease in nail patella syndrome. Nat Genet. 2001; 27:205–208. [PubMed: 11175791]
16. Kruse K, Kracht U. Evaluation of serum osteocalcin as an index of altered bone metabolism. Eur J Pediatr. 1986; 145:27–33. [PubMed: 3015628]
17. Fretz JA, Nelson T, Horowitz MC. Ebf1: An essental regulator of mysenchymal lineage allocation and osteoblast differentiation [abstract]. Journal of Bone and Mineral Research. 2011; 26:S457.
18. Cheung, aK; Manolagas, SC.; Catherwood, BD., et al. Determinants of serum 1,25(oh)2d levels in renal disease. Kidney Int. 1983; 24:104–109. [PubMed: 6604833]
19. Delmas PD, Wilson DM, Mann KG, et al. Effect of renal function on plasma levels of bone gla-protein. J Clin Endocrinol Metab. 1983; 57:1028–1030. [PubMed: 6604733]
20. Coen G, Mazzaferro S, Bonucci E, et al. Bone gla protein in predialysis chronic renal failure. Effects of 1,25(oh)2d3 administration in a long-term follow-up. Kidney Int. 1985; 28:783–790. [PubMed: 3878905]
21. Epstein S, Traberg H, Raja R, et al. Serum and dialysate osteocalcin levels in hemodialysis and peritoneal dialysis patients and after renal transplantation. J Clin Endocrinol Metab. 1985; 60:1253–1256. [PubMed: 3889031]
22. Sebert JL, Ruiz JC, Fournier A, et al. Plasma bone gla-protein: Assessment of its clinical value as an index of bone formation in hemodialyzed patients. Bone Miner. 1987; 2:21–27. [PubMed: 3509784]
23. Singer MA, Morton aR. Mouse to elephant: Biological scaling and kt/v. Am J Kidney Dis. 2000; 35:306–309. [PubMed: 10676731]
24. Shemesh O, Golbetz H, Kriss JP, et al. Limitations of creatinine as a filtration marker in glomerulopathic patients. Kidney Int. 1985; 28:830–838. [PubMed: 2418254]
25. Brunskill EW, Potter SS. Gene expression programs of mouse endothelial cells in kidney development and disease. PLoS One. 2010; 5:e12034. [PubMed: 20706631]
26. Visel A, Thaller C, Eichele G. Genepaint.Org: An atlas of gene expression patterns in the mouse embryo. Nucleic Acids Res. 2004; 32:D552–556. [PubMed: 14681479]
27. Vaughan MR, Quaggin SE. How do mesangial and endothelial cells form the glomerular tuft? J Am Soc Nephrol. 2008; 19:24–33. [PubMed: 18178797]
28. Lindahl P, Hellstrom M, Kalen M, et al. Paracrine pdgf-b/pdgf-rbeta signaling controls mesangial cell development in kidney glomeruli. Development. 1998; 125:3313–3322. [PubMed: 9693135]
29. Kikkawa Y, Virtanen I, Miner JH. Mesangial cells organize the glomerular capillaries by adhering to the g domain of laminin alpha5 in the glomerular basement membrane. J Cell Biol. 2003; 161:187–196. [PubMed: 12682087]
30. Miner JH. Developmental biology of glomerular basement membrane components. Curr Opin Nephrol Hypertens. 1998; 7:13–19. [PubMed: 9442357]
31. Noakes PG, Miner JH, Gautam M, et al. The renal glomerulus of mice lacking s-laminin/laminin beta 2: Nephrosis despite molecular compensation by laminin beta 1. Nat Genet. 1995; 10:400–406. [PubMed: 7670489]

32. Miner JH, Li C. Defective glomerulogenesis in the absence of laminin alpha5 demonstrates a developmental role for the kidney glomerular basement membrane. Dev Biol. 2000; 217:278–289. [PubMed: 10625553]
33. Kreidberg JA, Donovan MJ, Goldstein SL, et al. Alpha 3 beta 1 integrin has a crucial role in kidney and lung organogenesis. Development. 1996; 122:3537–3547. [PubMed: 8951069]
34. Kang JS, Wang XP, Miner JH, et al. Loss of alpha3/alpha4(iv) collagen from the glomerular basement membrane induces a strain-dependent isoform switch to alpha5alpha6(iv) collagen associated with longer renal survival in col4a3−/− alport mice. J Am Soc Nephrol. 2006; 17:1962–1969. [PubMed: 16769745]
35. Eremina V, Sood M, Haigh J, et al. Glomerular-specific alterations of vegf-a expression lead to distinct congenital and acquired renal diseases. J Clin Invest. 2003; 111:707–716. [PubMed: 12618525]
36. Kriz W. Ontogenetic development of the filtration barrier. Nephron Exp Nephrol. 2007; 106:e44–50. [PubMed: 17570939]
37. Fierlbeck W, Liu A, Coyle R, et al. Endothelial cell apoptosis during glomerular capillary lumen formation in vivo. J Am Soc Nephrol. 2003; 14:1349–1354. [PubMed: 12707404]
38. Ricono JM, Xu YC, Arar M, et al. Morphological insights into the origin of glomerular endothelial and mesangial cells and their precursors. J Histochem Cytochem. 2003; 51:141–150. [PubMed: 12533522]
39. Hanson J, Gorman J, Reese J, et al. Regulation of vascular endothelial growth factor, vegf, gene promoter by the tumor suppressor, wt1. Front Biosci. 2007; 12:2279–2290. [PubMed: 17127464]
40. Moffat, DB. The mamalian kidney. Cambridge University Press; Cambridge: 1975.
41. Norwood VF, Morham SG, Smithies O. Postnatal development and progression of renal dysplasia in cyclooxygenase-2 null mice. Kidney Int. 2000; 58:2291–2300. [PubMed: 11115063]
42. Komhoff M, Wang JL, Cheng HF, et al. Cyclooxygenase-2-selective inhibitors impair glomerulogenesis and renal cortical development. Kidney Int. 2000; 57:414–422. [PubMed: 10652018]
43. Benz K, Buttner M, Dittrich K, et al. Characterisation of renal immune cell infiltrates in children with nephrotic syndrome. Pediatr Nephrol. 2010; 25:1291–1298. [PubMed: 20386928]
44. Couser WG. Basic and translational concepts of immune-mediated glomerular diseases. J Am Soc Nephrol. 2012; 23:381–399. [PubMed: 22282593]
45. Quaggin SE, Vanden Heuvel GB, Igarashi P. Pod-1, a mesoderm-specific basic-helix-loop-helix protein expressed in mesenchymal and glomerular epithelial cells in the developing kidney. Mech Dev. 1998; 71:37–48. [PubMed: 9507058]
46. Miner JH, Morello R, Andrews KL, et al. Transcriptional induction of slit diaphragm genes by lmx1b is required in podocyte differentiation. J Clin Invest. 2002; 109:1065–1072. [PubMed: 11956244]
47. Rohr C, Prestel J, Heidet L, et al. The lim-homeodomain transcription factor lmx1b plays a crucial role in podocytes. J Clin Invest. 2002; 109:1073–1082. [PubMed: 11956245]
48. Cui S, Li C, Ema M, et al. Rapid isolation of glomeruli coupled with gene expression profiling identifies downstream targets in pod1 knockout mice. J Am Soc Nephrol. 2005; 16:3247–3255. [PubMed: 16207825]
49. Lin H, Grosschedl R. Failure of b-cell differentiation in mice lacking the transcription factor ebf. Nature. 1995; 376:263–267. [PubMed: 7542362]
50. Fretz JA, Nelson T, Xi Y, et al. Altered metabolism and lipodystrophy in the ebf1-deficient mouse. Endocrinology. 2009
51. Gundberg CM, Clough ME, Carpenter TO. Development and validation of a radioimmunoassay for mouse osteocalcin: Paradoxical response in the hyp mouse. Endocrinology. 1992; 130:1909–1915. [PubMed: 1547718]
52. Festa E, Fretz J, Berry R, et al. Adipocyte lineage cells contribute to the skin stem cell niche to drive hair cycling. Cell. 2011; 146:761–771. [PubMed: 21884937]

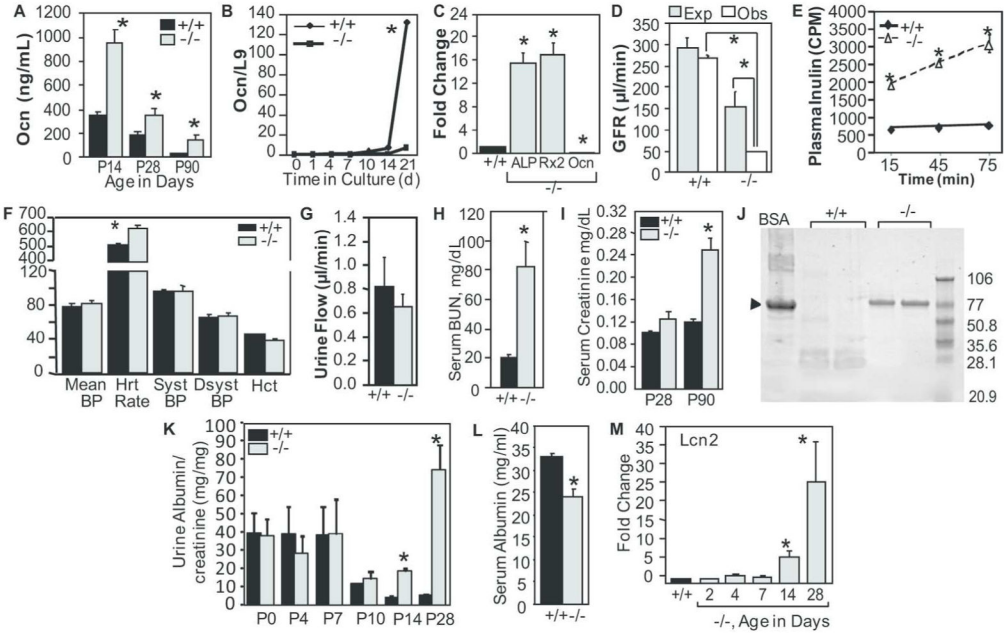

Fig. 1. GFR Is Reduced In *EBF1*$^{-/-}$ Mice And Accompanied By Albuminuria

A) Serum Ocn was measured in *Ebf1*$^{+/+}$ and *Ebf1*$^{-/-}$ mice at various ages. B) Calvarial osteoblasts were isolated from *Ebf1*$^{+/+}$ or $^{-/-}$ pups and cultured for the indicated times in the presence of osteoblastic differentiation media. RNA expression was examined with RT-qPCR and normalized to L9 transcript. C) Long bones were flushed of marrow and then assayed for the presence of message. Alkaline phosphatase (ALP) and Runx2 (Rx2) are early osteoblastic controls. D) GFR was measured in P56 mice (n = 8 *Ebf1*$^{+/+}$, 5 *Ebf1*$^{-/-}$). Measured GFR (Obs) is shown, as is the expected GFR (Exp) based on body size. E) Plasma inulin was measured in the bloodstream during the infusion. F) Vital signs were monitored during sedation and perfusion. They included heart rate (Hrt Rate), blood pressure (BP) (mean as well as systolic (Syst) and disystolic (Dsyst)), and hematocrit (Hct). G) Urine flow was also measured. H) BUN in serum from P28 animals (n = 5 mice per genotype). I) Serum Creatinine (n = 5 mice per genotype). J) SDS PAGE and comassie staining of urine from two separate P28 animals per genotype. Each lane was loaded with 1 µl of urine. Reference lane contains 10 ug of BSA as a sizing and loading control. K) Urinary albumin to creatinine ratio measured in mice of varying ages (n = 3–5 mice per genotype per age). L) Serum albumin was measured in the circulation of P28 animals. M) RNA expression of Lipocalin 2 (Lcn2) transcripts in whole kidneys. Values are first normalized to L9 and then expressed as a fold change of the age matched *Ebf1*$^{+/+}$ expression level. (n = 3–6 mice each). (*p ≤ 0.05)

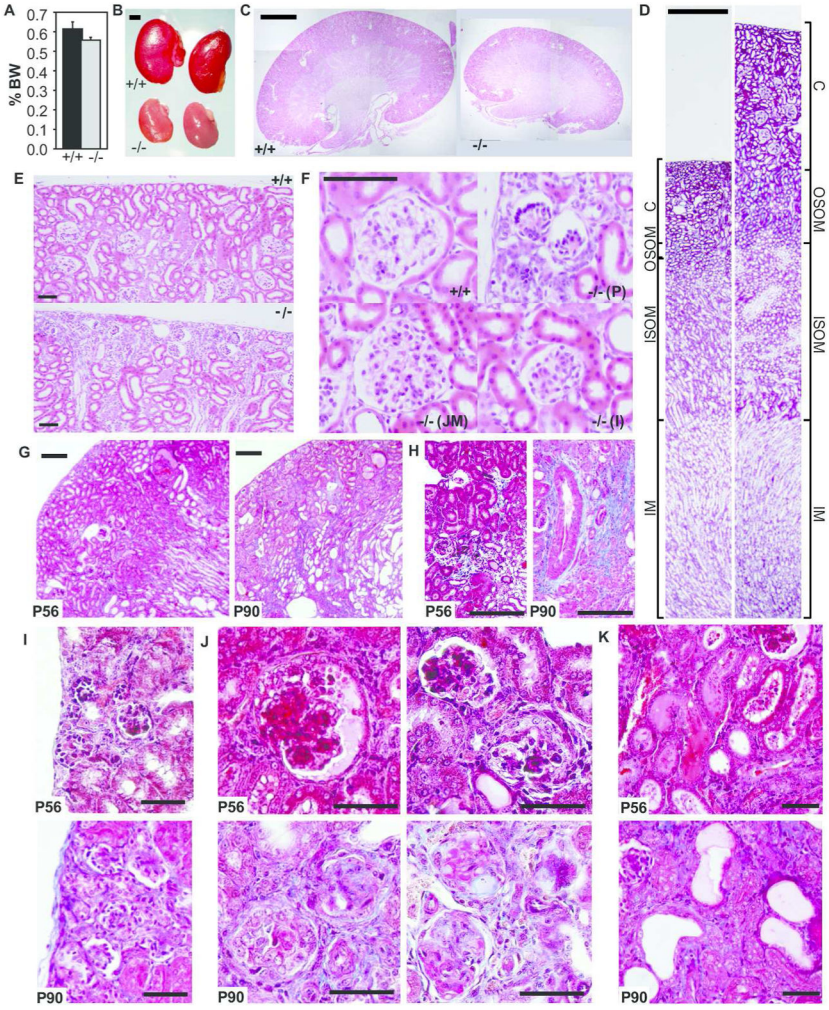

Fig. 2. Histological Examination of *EBF1*$^{-/-}$ Mice Kidney

A) Kidneys weights were recorded and expressed as a percent of total body weight. B) Representative kidneys from 4 separate mice are shown. Bar = 2 mm. C) H&E staining of perfusion-fixed kidneys from P28 *Ebf1*$^{+/+}$ and $^{-/-}$ animals. Bar = 2 mm. D) Trichrome staining of P28 perfusion-fixed kidneys. Bar = 300 μm. (C)- Cortex, (OSOM)- Outer stripe of the outer medulla, (ISOM)- Inner stripe of the outer medulla, (IM)- Inner medulla. E) Magnification of H&E stained peripheral cortex from P28 perfusion-fixed sections. Bar = 50 μm. F) Representative glomeruli are shown for each genotype in P28 H&E stained kidneys. Phenotype varies by cortex depth. (P)-Peripheral, (I)-Intermediate, (JM)- Juxtamedullary. Bar = 50 μm. G) Kidneys from P56 and P90 mice stained with Trichrome. Bar = 200 μm. H) Trichrome staining of interstitial immune infiltration present in P56 and P90 *Ebf1*$^{-/-}$ kidney. Bar = 200 μm. I) Persistent immature phenotype of peripherial glomeruli in P56 and P90 kidney. Bar = 50 μm. J) Phenotype of Trichrome stained JM glomeruli at P56 and P90. Bar = 50 μm. K) Tubular dilation with protein casts and schistocytes. Bar = 50 μm.

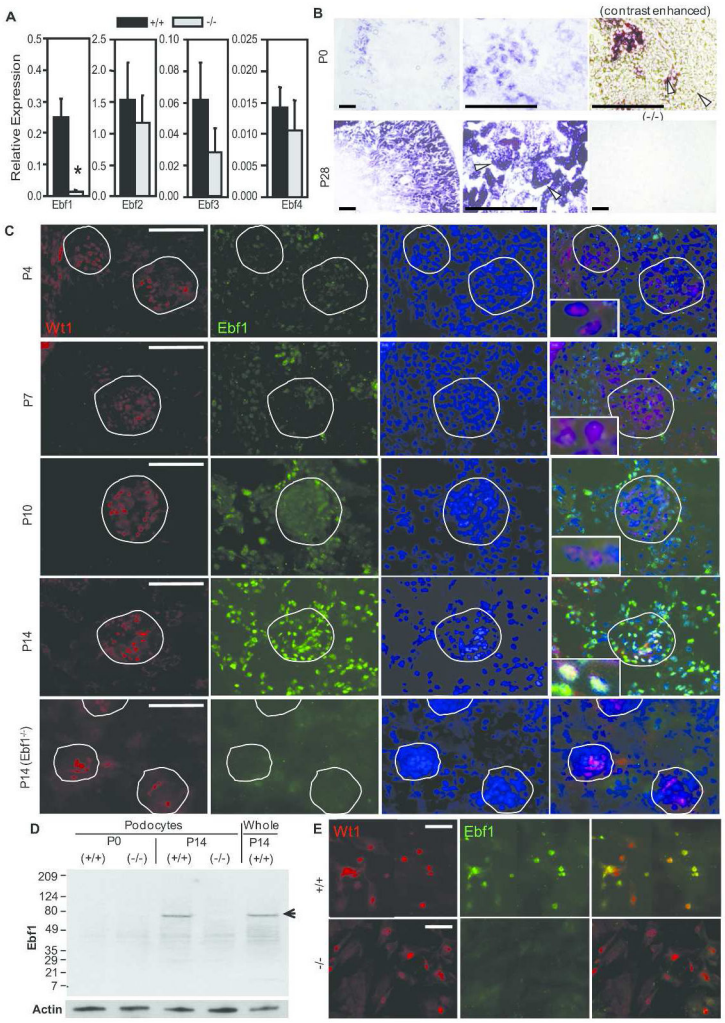

Fig. 3. Ebf1 Expression is Spatially and Temporally Regulated During Postnatal Kidney Development

A) Expression of Ebf-family transcripts by RT-qPCR in RNA isolated from P28 kidney. Values are normalized to the expression of L9 (n = 5–6 mice per genotype). (*$p \leq 0.05$) B) ISH of Ebf1 mRNA expression in neonate (P0) and P28 mice. Glomeruli are indicated with white arrowheads. $Ebf1^{-/-}$ control is shown to highlight specificity of the probe. Bar = 200 μm. C) IF of Ebf1 expression in glomeruli during postnatal development. Wt1 is used as a positive marker for podocytes. DAPI is used for nuclear counterstain. Merge is shown at far right with insets highlighting co-localization within podocyte nuclei. Glomeruli are outlined for orientation. Bar = 50 μm. D) Western blot for Ebf1 in cell lysate from primary podocytes isolated from P0 and P14 mice. Whole kidney is shown as a positive control. Actin is shown as a loading control. E) IF of Ebf1 expression in isolated podocytes. Wt1 is used as a positive marker for podocytes. Bar = 50 μm.

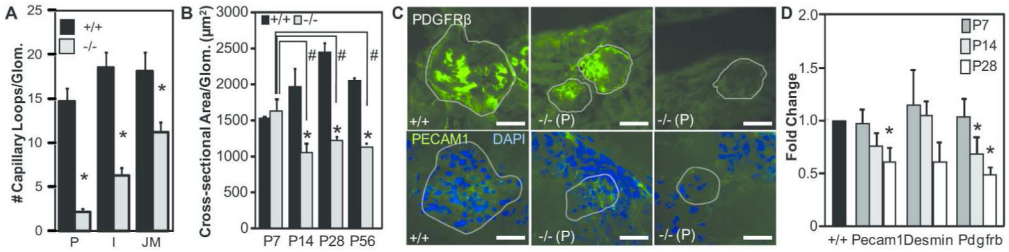

Fig. 4. Cortex Depth-Dependent Heterogenetity of Tuft Development

A) The number of capillary loops per glomeruli was quantified in 10–20 glomeruli per cortex location. (P)-Peripheral, (I)-Intermediate, (JM)- Juxtamedullary. B) Glomerular maturation was evaluated by quantifying the cross-sectional area per glomeruli for all glomeruli present in saggital sections of kidney. (n = 3 mice per genotype). C) IF of PDGFRβ (mesangial) and PECAM-1 (endothelial) in peripheral (P) glomeruli from P28 animals. DAPI is used as nuclear counterstain. Glomeruli are outlined for spatial orientation. Bar = 20 µm. D) RNA expression of mesangial (Desmin, Pdgfrb) and endothelial (Pecam1) markers in whole kidney. Values are first normalized to L9 and then expressed as a fold change of the age matched *Ebf1*$^{+/+}$ expression level. (n = 3–6 mice each). (*$p \leq 0.05$ compared to age matched control, #$p \leq 0.05$ compared to P7 value)

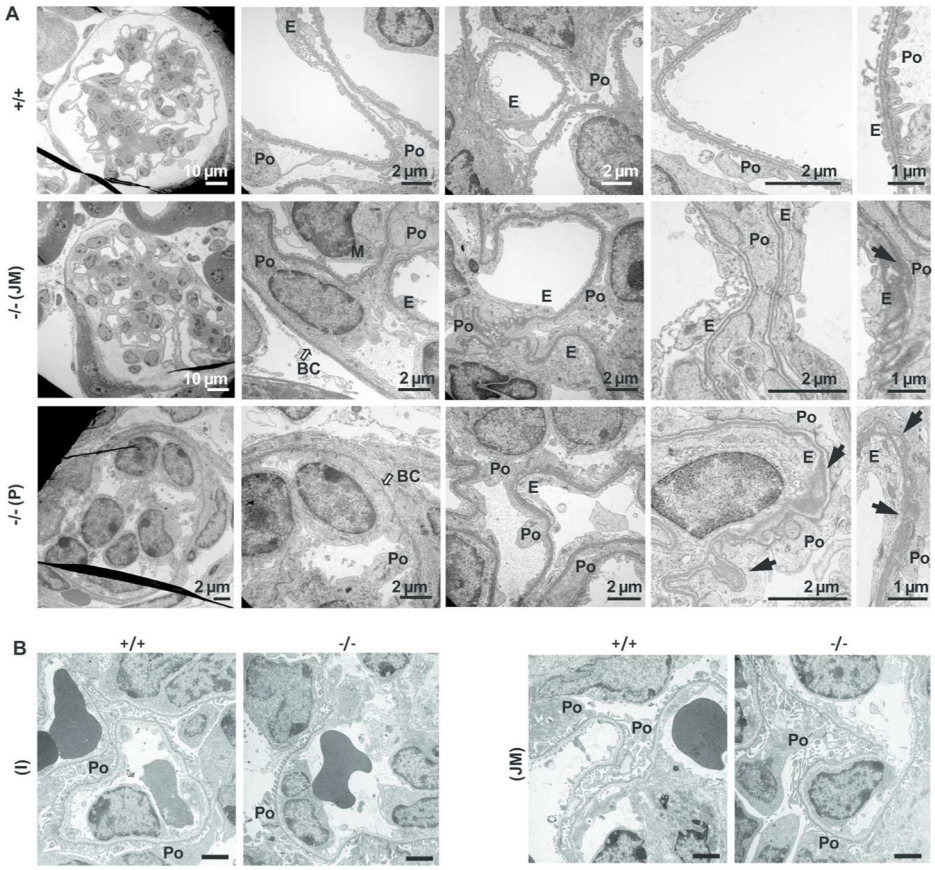

Fig. 5. EBF1$^{-/-}$ Podocytes are severely effaced with apical attachment to Bowman's capsule and localized defects in GBM

A) TEM from P28 animals. Representative glomeruli are shown. Due to the heterogeneity of phenotype dependent on cortex depth in the *Ebf1*$^{-/-}$ animals, cortex location and low power examples are provided. Basket weaving and separation of the GBM is highlighted with black arrows. BC= bowman's capsule (white arrows), Po=podocyte, E=endothelial cell, (P)-Peripheral, (JM)- Juxtamedullary. B) TEM was performed on kidneys of P0 neonates. Glomeruli in the juxtamedullary (JM) and Intermediate (I) regions of the cortex were visualized for podocyte foot process formation, GBM structure, and endothelial fenestration. Po= Podocyte. Bar = 2 µm.

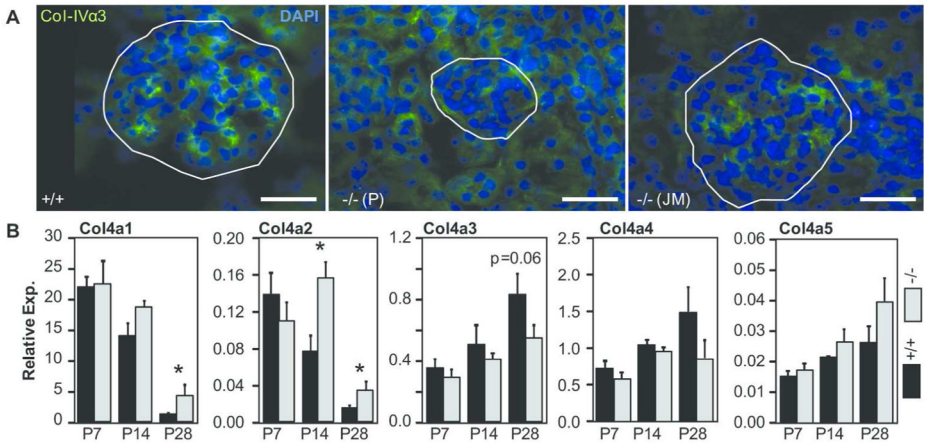

Fig. 6. Improper GBM maturation in Ebf1$^{-/-}$ Glomeruli

A) IF of Collagen IVα3 in P14 tissue. DAPI is used as nuclear counterstain. Glomeruli are outlined for spatial orientation. Bar = 20 μm. B) RNA from whole kidneys was used to examine transcript expression of GBM-associated collagens. Values are first normalized to L9 and then expressed as a fold change of the age matched *Ebf1*$^{+/+}$ expression level. (n = 3–6 mice each). (*p ≤ 0.05)

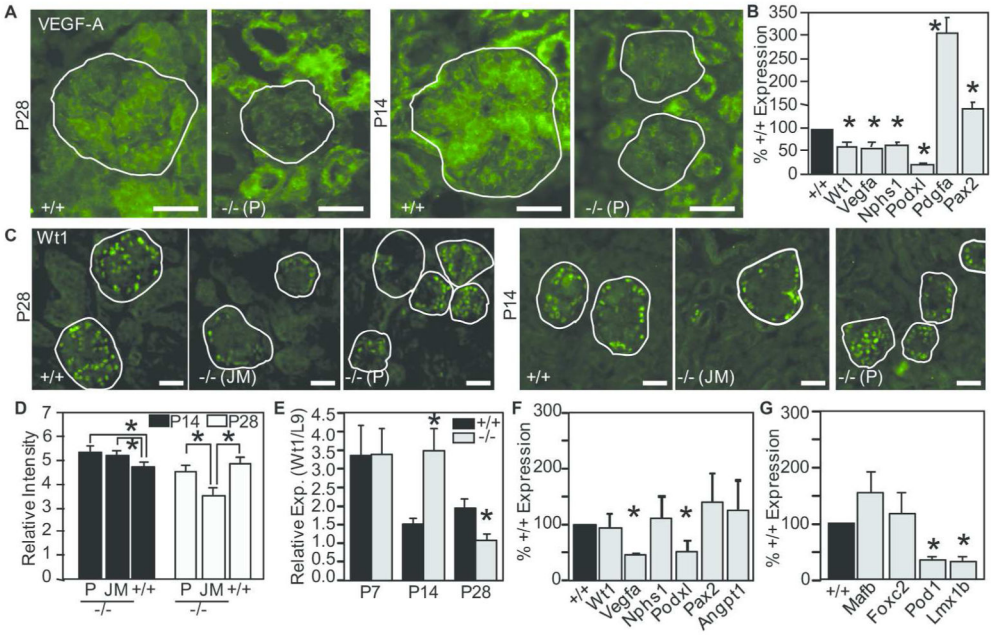

Fig. 7. Onset of the glomerular phenotype is accompanied by decreased VEGF-A

A) VEGF-A expression in glomeruli was examined by IF in P28 and P14 animals. Glomeruli are outlined. Bar = 20 μm. B) RT-qPCR examination of Wt1 and several Wt1 transcriptional targets (VEGF-A, Nephrin (Nphs1), Podocalyxin (Podxl), PDGFRα, and Pax2) in whole kidney from P28 *Ebf1*$^{-/-}$ mice. Values are normalized to L9 transcript expression and then expressed as fold change from the age matched *Ebf1*$^{+/+}$ tissue. C) IF of Wt1 in peripheral (P) and juxtamedullary (JM) glomeruli of P28 and P14 kidney. Bar = 20 μm. D) Quantification of IHC intensity for Wt1 expression in nuclei. At least 50 nuclei were analyzed per region and genotype. E) RT-qPCR examination of Wt1 in whole kidney of *Ebf1*$^{+/+}$ and $^{-/-}$ animals of various ages. F) RT-qPCR examination of Wt1, several Wt1 transcriptional targets, and angiopoietin-1(Angpt1) in isolated podocytes from P28 animals. Values are normalized to L9 and then expressed as fold change from the age matched *Ebf1*$^{+/+}$ tissue. G) RT-qPCR examination of other TFs important for podocyte maturation (Mafb, Foxc2, Pod1, Lmx1b) in isolated podocytes from P28 animals. Values are normalized to L9 transcript expression and then expressed as fold change from the age matched *Ebf1*$^{+/+}$ tissue. (*p ≤ 0.05)